

# Sequence Stratigraphy Interpretation at Callie Mine, Tanami Desert, Northern Territory

GEOSCIENCE AUSTRALIA  
PROFESSIONAL OPINION 2004/03

By

Lex Lambeck



**Australian Government**  
**Geoscience Australia**

**Geoscience Australia**

Chief Executive Officer: Dr Neil Williams

© Australian Government 2004

This work is copyright. Apart from any fair dealings for the purpose of study, research, criticism, or review, as permitted under the *Copyright Act 1968*, no part may be reproduced by any process without written permission. Copyright is the responsibility of the Chief Executive Officer, Geoscience Australia. Requests and enquires should be directed to the **Chief Executive Officer, Geoscience Australia, GPO Box 378 Canberra ACT 2601**.

Geoscience Australia has tried to make the information in this product as accurate as possible. However, it does not guarantee that the information is totally accurate or complete. Therefore, you should not solely rely on this information when making a commercial decision.

<p><b>Bibliographic reference:</b> Lambeck, A., Sequence Stratigraphy Interpretation at Callie Mine, Tanami Desert, Northern Territory. Geoscience Australia Professional Opinion 2004/03. 23pp.</p>
--

# Contents

<b>Abstract.....</b>	<b>1</b>
<b>Introduction .....</b>	<b>1</b>
<b>Regional Geology.....</b>	<b>1</b>
Gold Mineralisation .....	2
Local stratigraphy .....	3
<b>Methods.....</b>	<b>3</b>
<b>Results and Discussion.....</b>	<b>4</b>
Facies Trends .....	5
Geochemistry of the Tanami Basin.....	6
Downhole gamma, TiO <sub>2</sub> /Zr and vanadium values .....	7
Implications for ore genesis .....	7
Callie Boudin Chert.....	8
Downhole total organic carbon .....	8
Determination of tectonic setting of sandstones and mudstone suites .....	9
<b>Conclusions and proposed future work and techniques .....</b>	<b>10</b>
<b>Acknowledgements.....</b>	<b>11</b>
<b>References .....</b>	<b>11</b>
<b>Figures.....</b>	<b>13</b>

# Abstract

A pilot study of the Callie deposit was devised to test the application of sequence stratigraphy based techniques including continuous grainsize curves, identification of sedimentary structures, and geochemical data to identify favourable horizons for gold mineralisation. This study highlights novel applications of several geochemical proxies. The location of ore-bearing beds within the sequence is identified with downhole curves for total organic carbon, vanadium,  $\text{TiO}_2/\text{Zr}$ , and a proxy gamma curve. The proxy gamma curve was generated by combining concentrations of potassium, uranium and thorium. These geochemical proxies are supplemented with lithologic and grainsize data to identify and interpret stratal surfaces. The ore is hosted in a condensed section containing a number of higher order flooding surfaces which are highlighted by fine grained black carbonaceous units and high values for geochemical proxies. As a result of this pilot study this research will be further expanded to incorporate the north and west of the Tanami region and further constrain basin extent and evolution. This will form a necessary stepping stone to formulating models aimed at constraining fluid flow into the Tanami Region.

## Introduction

The Tanami region in the Northern Territory and Western Australia hosts the world-class Callie gold mine in the Dead Bullock Soak (DBS) goldfield approximately 550 km northwest of Alice Springs. The finding of a world-class deposit at Callie has led to continuing exploration and development of the area. Due in part to the high proportion of cover in the region, the need has risen to synthesise known mine geology and generate new predictive tools for future exploration.

Sequence stratigraphic concepts provide a methodology for recognising surfaces of chronostratigraphic significance in a sedimentary basin. The approach used herein combines mineral and petroleum exploration techniques focusing on a number of key concepts such as grainsize and major and trace element geochemistry. As ore commonly occurs in fine grained carbonaceous black shales in the Tanami Region one of the main purposes of this study is to construct a model to determine basin architecture and understand geochemical indicators within the black shales. The results of this study place the mine stratigraphy in a new geologic framework and can supplement existing geology to identify traps and vectors towards traps that cause gold to precipitate.

Sequence stratigraphy relies on the integration of seismic, outcrop, drill hole and wire-line logs to provide an understanding of basin architecture. An absence of seismic data coupled with poor exposure has resulted in the need to integrate the drill core logs from relatively shallow exploration holes to construct a 'composite' section of the stratigraphy at Dead Bullock Soak. All the Geology and geochemical data are included in the CD.

## Regional Geology

The world-class Callie gold mine located in the Dead Bullock Soak (DBS) goldfield is one of several gold deposits in the Tanami Region including The Granites, 40 km east of DBS, Titania, 20 km north of DBS and Groundrush deposit 100km north of the Granites (Figure 1). The deposits are hosted in a range of rock types and vary in size and style. Callie is by far the largest deposit in the region with gold occurring as nuggets within extensive thin sheeted quartz veins hosted by metasediment of greenschist facies.



The Tanami region consists of a complex sequence of folded and faulted metasediments. Hendrickx et al. (2000) and Vanderberg et al. (2001) have described the geology, stratigraphy, and structure of the Tanami Region in detail. A brief review of the regional geology, stratigraphy, gold mineralisation and mine nomenclature at Callie are provided in Table 1 and below.

The Tanami Group metasediments overlie basement rocks along a fault-bounded contact. Basement in the region is inferred to be Archaean banded granitic gneisses of the Billabong Complex (Cooper and Ding, 1997), however these rocks do not outcrop near DBS. The Tanami Group comprises two formations, the lower Dead Bullock Formation and overlying Killi Killi Formation (Table 1).

The Dead Bullock Formation incorporates the informally named Blake Beds and Davidson Beds of Smith et al. (1998) as well as the MacFarlane Peak Group and Twigg Formation of Hendrickx et al. (2000). The unit has been subdivided by Crispe and Vanderberg (2004) into two members; the lower Ferdies member, comprises feldspathic sandstone, fine grained sandstone often interbedded with siltstone, and the upper Callie Member, comprising fine grained lithologies, siltstone, chert, iron-rich siltstone and shale. Ferdies Member is equivalent to most of the Lower Blake Beds and Callie Member is broadly equivalent to the Upper Blake Beds and Davidson Beds of Smith et al (1998).

The Dead Bullock Formation, DBF, is a deep-water, fining upwards succession in which fine sandstone, siltstone and carbonaceous siltstone grade into chert-bearing banded iron formation and shale. The base of the DBF is not observed in any of the cores. However, observations by Newmont NFM geologists indicate that lithic sandstone displaying soft sediment deformation and intraformational breccias underlies the exposed sequence at Dead Bullock Soak. The overlying Killi Killi Formation is a thick monotonous package of turbiditic sandstone and siltstone. This formation forms the upper unit of the Tanami Group, representing the last episode of sedimentation prior to the Tanami Orogenic Event at ~1840-1825 Ma (Vanderberg et al., 2001). The Tanami Group is intruded by 1825-1790 Ma granitic suites and numerous foliated dolerite sills; the ages of the sills are generally poorly constrained. Most of the intrusives are foliated and hence pre-date major deformation in the region.

The Tanami Group is interpreted as a predominantly deep-water transgressive-regressive package. Fine grained sediment dominates the DBF which accumulated in relatively deep water beneath below storm wave base. Coarser grained and thicker bedded rhythmites of the Killi Killi Formation provide evidence of an encroaching sediment source and regression.

The DBF is tentatively inferred to be deposited between 1880-1850 Ma based on similar lithology to the Koolpin Formation at Pine Creek and Biscay Formation at Halls Creek. The younger Killi Killi Formation is inferred to be deposited after 1840 Ma (Crispe et al., 2002) based on detrital zircon and granite ages.

## Gold Mineralisation

Since modern exploration in the 1980's in the Tanami region, a number of discoveries have been made and the Tanami has now emerged as one of Australia's most prospective and productive gold provinces.

Crispe and Vandenberg (2004) have classified gold mineralisation into two broad categories:

- 1) Shallow level, epizonal mineralisation characterised by the deposits of the Tanami corridor, including Galifrey, Crusade and Pendragon deposits.
- 2) Deep level, meso-thermal mineralisation, which can be subdivided on mineralisation type into:



- A) The Granites-style – hosted by iron formations, *e.g.* The Granites goldfields, some DBS deposits, Horden Hills and Minotaur deposits.
- B) Callie-style – hosted by decarbonised siltstone, *e.g.* Callie, Gahn and Titania deposits
- C) Groundrush-style – hosted by a metamorphosed mafic sill, of which there is only one example.

This study only addresses Callie-style deposition, concentrating on the metasediments that host the ore with the aim of developing a better understanding of basin architecture and geochemistry of the stratigraphy. Similar techniques will be used at the Granites, Groundrush, Titania and Coyote to further understand the basin architecture of the Tanami region.

## Local Stratigraphy, Dead Bullock Soak

Smith et al. (1998) first described the informal subdivision of the Dead Bullock Formation which is further described by Emslie and Voulgaris (2004). All the units at DBS have undergone greenschist facies metamorphism and they are described briefly in Table 1. The unit thickness information on the Geologs is provided from Emslie (*pers. comm.*, 2003). The distinction between the Blake, Davidson and Madigan Beds is made on chemical signatures and sedimentary features. The grainsize fines up through the Lower Blake Beds and Lower Blake Laminations into fine black graphitic and non-graphitic sediments of the Callie Laminated Beds, Magpie Schist and Callie Boudin Chert. The sediment then slowly coarsens up from silt to fine sand through the Davidson Beds into the Madigan Beds as seen in Table 1 and Figure 2.

## Methodology

This project involved two weeks of field work at the Callie mine logging and sampling core from five diamond drill holes. Cores were selected that were the least mineralised with minimum recorded fault zones. Sedimentary facies characteristics such as grainsize, lithology, sedimentary structures and grain composition were tabulated for each core on field data sheets. Grainsize information was collected as a continuous curve. Representative samples for geochemistry were taken approximately every 5 metres. Care was taken to keep the sample suite to a manageable size for the laboratory work but, if the lithology changed markedly within 5 metres another sample was taken.

Drill cores were selected in close consultation with Newmont mine staff using known mine stratigraphy and structural data. The five diamond cores were combined to provide a composite core of the DBS region as no one core at DBS passes through the entire stratigraphy. The relative order of the composite core relies entirely on Newmont stratigraphy because the relationship between the individual cores is not fully known.

Whole rock major and trace element analysis was performed on 280 samples in two batches. The first batch of 62 samples were split pulp samples crushed in a tool steel mill by Newmont. The second batch consisted of hand samples, 50-300gm, prepared in a tungsten-carbide mill and a tool steel mill within Geoscience Australia. Major and trace element analysis were performed at Geoscience Australia's geochemical laboratory using a Perkin Elmer Elan 6000 ICP-MS in conjunction with the methods of Jenner et al. (1990) and Pyke (2000), or a Phillips PW2404 4k W sequential X-ray fluorescence (XRF) spectrometer following the methods of Norrish and Chappell (1977).

In the absence of downhole, wireline-derived gamma-ray data it was necessary to use geochemical techniques to derive a 'proxy gamma' curve. Total potassium, uranium and thorium



from whole rock geochemistry were combined to give a Gamma Dosage Rate as detailed by UNSCEAR (1988) and results plotted as a gamma ray curve for comparison with grain size facies. The  $\text{TiO}_2/\text{Zr}$  ratio and vanadium concentrations are also illustrated as a downhole plot to highlight potentially mineralised horizons.

Seventeen samples were selected for total organic carbon (TOC) to identify possible relationships between facies and TOC in these Palaeoproterozoic samples. Crushed samples were prepared as detailed in Peters (1986) using the RockEval 6 Turbo, Vinci Technologies.

Techniques for calculating true thickness for each lithological unit still need to be developed. Currently each unit in the DBD-Composite log has been compressed to estimated mine thicknesses as advised by Emslie (pers. comm., 2003). To better understand how units thin and thicken laterally a new technique for calculating true thickness will need to be developed.

## Results and Discussion

Figure 2 graphically shows variation in grain size, sedimentary structures and geochemistry for all cores logged. The individual and composite logs are also presented in the accompanying CD. Table 1 summarizes the unit descriptions, stratigraphic interpretation and abbreviated stratigraphy nomenclature. As the Pip Schist was not logged in 2003, it was not included in Figure 2 and Table 1. This unit will be logged in July 2004.

### *Lithological description: DBD0419*

From bottom to top drill hole DBD0419 intersects LBB interfingering with LBL which grades into CLB. Throughout the core the units are cut by numerous dolerites.

The sediment represents an overall fining upwards sequence, from the LBB consisting of a meta-sandy siltstone grading into the CLB consisting of a black graphitic meta-mudstone (see Geolog DBD0419). Only a section of DBD0419 has been logged. The lower parts of this hole which intersect the LBB will be logged in 2004.

### *Lithological description: DBD0440*

From bottom to top drill hole DBD0440 intersects CLB and grades into MS, CBC and UBB with one small interval of DBM. The sediment displays a subtle fining upwards trend from siltstone dominated facies of the CLB into black graphitic meta-mudstones and shales of the Upper Blake Beds. Black graphitic meta-mudstones of the Callie Laminated Beds, Magpie Schist Callie Boudin Chert and Upper Blake Beds represent the deepest water facies with tiny 'starvation ripples' observed between 670 m and 710 m indicating limited sediment input (see Geolog DBD0440).

### *Lithological description: DBD0431*

From bottom to top drill hole DBD0431 intersects UBB and grades into ORAC Formation made up of the LOC, MOS, LOC and UOC. The End It All Dolerite intrudes roughly parallel to bedding. DBD0431 drill core represents a shale unit, black graphitic meta-mudstone with little variation in grain size. The sediments are occasionally punctuated by chert. Silt horizons occur randomly throughout the unit (see Geolog DBD0431).

### *Lithological description: DBD0437*

From bottom to top, drill hole DBD0437 intersects DBM, SHIM and CS and is intruded by basic intrusives. Two tuffaceous units are noted in company logs. Geochemistry of these units is consistent with a mafic origin (Appendix A, on CD provided).

DBD0437 drill core represents a shale unit, black graphitic meta-mudstone, with scattered fine silt laminations (see Geolog DBD0437).



*Lithological description: DBD0434*

From bottom to top drill hole DBD0434 contains entirely Madigan Beds. The lower half of the drill core intersects a series of cycles of fining upward trends grading from fine sandstone to shale over 15 cm to 2 m. The higher part of the log consists mainly of fine sand to sandy silt (see Geolog DBD0434).

**Facies Trends**

*DBD0419: Transgression*

The fining upward trend in grainsize in DBD0419 suggests that water depth steadily increased, inferring a marine transgression. This interpretation is supported by an increasing content of carbonaceous material towards the top of the hole. It is noted that while mineralised sections of the core appear black and carbonaceous indicating an anoxic environment, they have low gamma values. This observation is attributed to silicification which may have replaced the clay fraction.

While every attempt was made to avoid mineralised cores it was noted that gamma values were low in the core. DBD0419 drill core has high vanadium and  $\text{TiO}_2/\text{Zr}$  values that correspond to the mineralised zones suggesting that gamma, vanadium and  $\text{TiO}_2/\text{Zr}$  values need to be measured in conjunction to highlight areas of possible mineralisation, (see Geolog DBD0419, Figure 2, Tables 1, 2).

*DBD0440: Transgression/Aggradation*

Drill core DBD0440 is inferred to lie stratigraphically above drill core DBD0419 and is interpreted as a continuation of the marine transgression. The subtle upwards fining trend, grading from predominately siltstone into claystone, and then black carbonaceous material suggests that the entire drill core represents a gradual reduction in siliciclastic flux. The top of drill core DBD0440 is a monotonous interval of black carbonaceous siltstone representing a condensed section. The relatively high gamma and high values of vanadium and  $\text{TiO}_2/\text{Zr}$  help highlight the fine-grained, unmineralised, non-silicified nature of the core. The lack of coarse material suggests that sedimentation took place in a deep water environment below storm wave base. The presence of starvation ripples support the notion that the basin is receiving very little sediment input, and preservation of black carbonaceous material indicates an anoxic depositional environment. Towards the middle of the core the sediments display a monotonous aggradational stacking of facies indicative of a deep-water condensed interval. (see Geolog DBD0440, Figure 2, Tables 1, 2). CLB and MS in the drill core have low gamma values and relatively high  $\text{TiO}_2/\text{Zr}$  and vanadium values which as in drill core DBD0419 are attributed to alteration.

The core is cut by a number of small faults, however little movement was inferred as the units do not change across the faults. However Whittaker (pers. comm., 2004) suggests that movement may be more significant and possible structural repetition will be investigated in the 2004 field session. At this point relatively minor fault repetition is not inferred to alter the conclusions of this report.

*DBD0431: Aggradation*

Drill core DBD0431 also represents a deep water environment with a lack of coarse material. Monotonous cyclic and rhythmic stacking of fine-grained black carbonaceous material indicates that aggradation is still occurring. The gamma values are marginally lower than the sediments from DBD0440 but are paired with relatively higher vanadium and  $\text{TiO}_2/\text{Zr}$  values. Individual peaks in the gamma, vanadium and  $\text{TiO}_2/\text{Zr}$  values are thought to highlight fine-grained, carbonaceous units within the ORAC formation. Possible distal turbidites are observed as silt horizons occurring randomly throughout the core. The End It All Dolerite also cuts the ORAC Formation roughly parallel to bedding, (see Geolog DBD0431, Figure 2, Tables 1, 2).

*DBD0437: Aggradation*

Core DBD0437 is also considered to represent a continuation of the condensed section. A monotonous cyclic and rhythmic stacking of fine sediment indicates that aggradation is still





occurring. The gamma, vanadium and  $\text{TiO}_2/\text{Zr}$  are all highly variable. The high values are interpreted to highlight the fine-grained carbonaceous SHIM horizons with the lower units representing the coarser units and potentially unmineralized zones, (see Geolog DBD0437, Figure 2, Tables 1, 2).

#### *DBD0434: Progradation*

The lower half of drill core DBD0434 is formed by turbidites which consist of a series of fining upward cycles that grade from fine sandstone to shale. An erosional surface can be placed between each turbidite because fine material is removed each time a new turbidite is formed. The fine sand to sandy silt in the top part of the drill core suggests a shallowing and the commencement of progradation. The gamma curve is highly variable and this is partly attributed to the highly variable grainsize curve. The vanadium and  $\text{TiO}_2/\text{Zr}$  curves generally mirror the gamma curve. The core is cut by a number of small faults however little movement is inferred as the units do not change noticeably across the fault zones, (see Geolog DBD0434, Figure 2, Tables 1, 2).

#### **Geochemistry of the Tanami Basin**

To enable a direct comparison, all analyses have been recalculated to 100% volatile-free and all samples containing greater than 5% carbonate and greater than 5% loss of ignition were removed. The data cluster in four distinctive geochemical and lithologic groups, that correlate with mine stratigraphy. For all geochemical data see Appendix B on the CD provided.

The four distinctive groups are: 1) the basal group, which includes the LBL, LBB, CLB, MS, CBC and UBB; 2) the ORAC group, which includes the LOC, MOS, UOC, and UOS; 3) the SHIM group, which includes the DBM, SHIM, CS, MC and SSS; and 4) the Madigan group, which is the highest group in the stratigraphy and comprises the Madigan Beds (Tables 3, 4). Small but systematic differences in trace element chemistry are observed between these groups of sediment. Examples of changing geochemistry downhole are highlighted and discussed below.

#### *Selected major and trace elements*

Traditionally, all elements and traces are plotted versus  $\text{SiO}_2$  to gain an understanding of provenance but at Callie  $\text{SiO}_2$  was mobilized by post-depositional fluid flow that produced numerous quartz veins. So chemical species plotted to  $\text{SiO}_2$  may not give appropriate geochemical signatures. Figures 3 and 4 show less mobile chemical species such as chromium, nickel, scandium, vanadium, magnesium oxide, titanium oxide and total iron plotted relative to both silica and zirconium. The concentrations of these elements from the Madigan and SHIM groups are substantially lower than the ORAC and LBB-UBB groups, but more typical of average post Archaean shales (Taylor and McLennan (1985). This may indicate a more primitive provenance for the ORAC and LBB-UBB groups. The Madigan and SHIM groups generally have a narrow concentration range of these elements although they show a greater range in silica content in comparison to the ORAC and LBB-UBB groups. This reflects the presence of coarser-grained lithologies in the Madigan and SHIM groups. Zirconium at Callie is considered to be immobile and is found to better resemble the traditional trace element versus silica plots. If an area is observed to have possible mobile silica, zirconium can be used as a substitute for silica to provide suitable plots. Average, maximum, minimum and standard deviations are shown in Table 4.

Figures 3 and 4 illustrate that there are four different horizons found within at DBS. These results suggest that the Newmont stratigraphy is accurate because each major lithologic unit appears to have different geochemical attributes. The basal section, LBB-UBB, marks a marine transgression and has distinctive geochemistry in comparison to the topmost unit, Madigan Beds. The Madigan Beds suggest progradation and are suggestive of sediments proximal to a basin fan system. Between the LBB-UBB and Madigan horizons are two units the, SHIM and ORAC groups forming part of an aggradational package, crosscut by the Cora Dolerite. The bottom two groups, LBB-UBB and ORAC, have similar geochemical characteristics and the top two groups,



SHIM and Madigan, share similar geochemical characteristics. The stratigraphic change in geochemistry could indicate a switch in the basin fan providing sediment to the basin.

#### **Downhole gamma, $\text{TiO}_2/\text{Zr}$ and vanadium plots**

The gamma, downhole  $\text{TiO}_2/\text{Zr}$  ratio and downhole vanadium values are used to help highlight the fine grained carbonaceous units which generally host ore at Callie. As potassium, uranium and thorium are found to be concentrated in clay fraction of rock, theoretical gamma dose rates can be calculated from chemical concentrations as described by UNSEAR (1988). The gamma curve shown in the logs provided is therefore a proxy gamma curve. While exact values from this curve are not directly analogous to wireline logs used in the petroleum industry, the same general trends can be expected.

Wyborn et al. (1983) using the chemistry of Ordovician and Silurian greywackes in the Snowy Mountains showed that there was a strong negative correlation between silica, and those elements which can be accommodated in the clay-bearing matrix such as titanium and vanadium. Therefore vanadium and gamma values may help highlight the fine clay fraction in the cores. The  $\text{TiO}_2/\text{Zr}$  ratio is used in the logs because these elements at Callie are generally thought to be less mobile, or immobile elements, and as such changes in  $\text{TiO}_2/\text{Zr}$  can be attributed to changing geochemistry in the basin at the time of deposition.

Each drill core log has a gamma,  $\text{TiO}_2/\text{Zr}$  and a vanadium curves plotted downhole, which help to highlight the fine-grained material and hence possible mineralised zones. While these curves provide a good visual aid to distinguishing broad overall changes in downhole geochemistry, perhaps a clearer way of interpreting this data is through the use of X-Y scatter plots. The data in Figure 5 shows the  $\text{TiO}_2/\text{Zr}$  ratio and vanadium plotted to gamma for the four groups as defined above.

Gamma versus  $\text{TiO}_2/\text{Zr}$  and vanadium plots show a distinctive bipartite distribution with the Madigan group and SHIM group having lower  $\text{TiO}_2/\text{Zr}$  and vanadium values than the ORAC and LBB-UBB groups. The stratigraphic change in geochemistry could again indicate a switch in the basin fan providing sediment to the basin. The grouping in Figure 5 confirms the Newmont stratigraphy and suggests no fault repetitions occur between the major units. Averages, maximums, minimums and standard deviations are shown in Table 2.

#### **Implications for ore genesis**

The integrated geochemical facies and sequence stratigraphy approach has important implications for ore genesis. The highest grade gold occurs in the well bedded carbonaceous horizons occurring in the condensed interval of the Lower Blake Beds; Callie laminated Beds and Magpie Schist. The condensed interval represents an anoxic environment and forms a chemical trap to the ore fluids as suggested by Williams (2002).

Fluid travelled along  $D_5$  shears and deposited gold when condensed sections were encountered. The Blake and Davidson Beds are aggradational deep water facies that represent a condensed interval. These beds may contain higher order maximum flooding surfaces which contain significantly mineralised units.

#### **Callie Boudin Chert**

The Callie Boudin Chert, which comprises carbonaceous mudstone with extensive bands of chert nodules up to 5 cm in diameter forms an enigmatic marker bed at the Callie Mine. These nodules are found in greatest numbers and size at the Callie Boudin Chert, they are also found in the ORAC and SHIM horizons. Based on similarities with nodules and concretions in deeper water successions elsewhere in the world (Clayton, 1986; Coniglio, 1987; Knauth, 1979), the nodules are interpreted to be of sedimentary origin formed in deep water, below storm wave base. Concentric growth rings within the nodules and enveloping laminations that are compacted around the nodules suggest that these features formed during early diagenesis. The nodules also



contain later evidence for shearing and folding and they have possibly been affected by later boudinaging (Smith et al. 1998)

The controls on nodule or concretions growth are an unresolved dilemma (Hesse 1990). Clayton (1986) uses an analogue between chalk and flint formations in the Cretaceous cliffs of England and proposes a general model for the formation of Precambrian cherts. The transition from anoxic to oxic conditions is interpreted to coincide with the cemented chalk/flint boundaries and the flint bands mark the position of the redox boundary which separates an oxic (above) from an anoxic environment (below) at the time of silica precipitation, (Figure 6). Coniglio (1987) found that silica precipitation can occur very early in diagenesis in the Cow Head (Cambro-Ordovician), western Newfoundland as evidenced by compacted, silicified shale draping earlier-formed limestone nodules. This is a feature shared with Knauth's (1979) model who postulated that burial depth at the time of silicification may have been as little as 5-10 m.

The banding of the nodules within the core can again be likened to the work of Clayton (1986) who suggests the rhythmic bedding of the chalk, exhibited by the regularly spaced flint bands in many coastal cliff sections may then reflect abrupt, stepwise rises of the redox-boundary related to basin-wide sedimentation pulses and/or breaks. Using this analogy the nodules found at DBS could have formed during periods of low sediment input into the basin. The distinct nodular banding found within black carbonaceous units of the CBC could be attributed to low levels of sedimentation into the basin as could the banding found within the SHIM and ORAC horizons. When looking at the composite log, nodules are observed throughout the section, excluding the Madigan Beds. Therefore the entire log could be attributed to a major condensed section with smaller higher order condensed sections forming at the CBC, ORAC and SHIM horizons. Because these nodules occur in multiple horizons and in multiple formations they should not be relied upon as definitive stratigraphic marker beds.

### **Downhole Total Organic Carbon**

Most sedimentary rocks of Precambrian age contain at least a small amount of organic matter that consists of the preserved residue of plant or animal tissue. The average content of organic matter in sedimentary rocks is 2.1 weight percent in shales, 0.29 in limestone's, and 0.05 percent in sandstones (Degens, 1965). The average content of organic matter in all sedimentary rocks is about 1.5 percent. Organic matter contains about 50-60 percent carbon, therefore the average sedimentary rock contains about 1 percent total organic carbon (TOC). A few special types of sedimentary rocks contain significantly more organic material than these average rocks. Black shales typically contain 3 to 10% TOC.

TOC was measured on 17 samples, 10 samples from DBD0434 and 7 samples from DBD0440. The 10 samples from DBD0434 returned low TOC values ranging between 0.01 – 0.52 %. These samples are lighter in colour compared to samples from DBD0440 which has overall higher TOC. This can be attributed to the rapid basin infilling with the deposition of the Madigan Beds and carbon oxidation prevented preservation of any TOC present. The 7 samples from DBD0440 taken from a siltstone grading into a black carbonaceous unit show a distinct correlation between observed colour and recorded TOC samples ranging from 0.04% TOC for rocks with a dull grey colour to 3.3% TOC for deep black colour. TOC is highly correlated to gamma (Figure 7) and thus TOC can be used to determine the placement of carbonaceous shales within condensed sections and hence potentially mineralised units.

Williams (2002) suggested the carbon ratio can decrease due to the removal of graphite by a relatively oxidised ore-bearing fluid. As mineralised units are approached the carbon values drop, and gamma counts will potentially rise due to mobile potassium associated with mineralisation. The hypothetical mineralisation window is depicted in the shaded area of Figure 7, where samples of lower TOC and higher gamma would plot.



### **Determination of tectonic setting of sandstone and mudstone suites**

Preliminary analysis suggests that the geochemistry of the Callie sequence can be used to infer the tectonic setting and provenance of the sediments. Tectonic activity on a range of scales is a fundamental control on sedimentary activity. The range of structural deformation within a region extends from a plate tectonic scale, *e.g.* initiation of rifts, to basin scale, with the formation of basin bounding faults. The relationship between tectonic activity and sedimentation is a very complex one due to the number of variables which influence sedimentary activity including: erosion, sediment transport style, source area, lithology, groundwater chemistry, and depositional environments.

Diagenesis can alter original geochemistry yet these changes may be related to plate tectonic environments. Bulk composition will still reflect tectonic setting and so enable bulk geochemistry to enable development of chemically-based discriminants to elucidate tectonic environments. The relationship between geochemistry of sedimentary rocks and tectonic setting has been extensively studied (Middleton, 1960; Crook, 1974; Bhatia, 1983; Bhatia and Crook, 1985; Roser and Korsch, 1986; Roser et al., 2002).

Roser and Korsch (1986) used geochemistry of sandstones and shales from inferred tectonic settings in New Zealand based on  $\text{SiO}_2$  content and  $\text{K}_2\text{O}/\text{Na}_2\text{O}$ . This study used individual data rather than averages to highlight any possible trends and concluded that the reflection of provenance in chemistry can be effectively broken into three broad categories: passive margin, active continental margin and oceanic island arc. Roser and Korsch (1986) use data from modern sediments and known tectonic settings to further test the general discriminant fields proposed. It should also be stressed that within each of the three broad divisions several depositional settings are possible. The categories defined by Roser and Korsch (1986) and used in this study are:

#### **1) Passive Continental Margin (PM)**

Mineralogically mature (quartz-rich) sediments deposited in plate interiors away from active plate boundaries. Sediments are deposited within stable continental margins and basins associated with ocean floor spreading, failed rifts and Atlantic-type continental margins.

#### **2) Active Continental Margin (ACM)**

Quartz-intermediate sediments derived from tectonically active continental margins on or adjacent to active plate boundaries. This category includes complex active margins including material derived from continental margin magmatic arcs deposited in a variety of basin settings including trench, forearc, intraarc and backarc basins as well as material derived from uplifted areas associated with strike-slip faults and deposited in pull-apart basins.

#### **3) Oceanic Island Arc (ARC)**

Quartz-poor volcanogenic sediments derived from oceanic island arc sources and deposited in a variety of settings including forearc, intra-arc and backarc basins and trenches.

The categories defined reflect the composition of rocks in source areas. However, care is needed when assessing the tectonic setting of sediments deposited in basins related to active plate boundaries because these basins (trench, forearc, intraarc, backarc) can be related to either continental margin magmatic arc (ACM) or an island arc (ARC).

Using the Roser and Korsch (1986) categorization, the Madigan Beds and SHIM are indicative of a passive margin setting. In contrast, ORAC and LBB-UBB groups range from passive margin, through oceanic island arc (Figure 8), with most data in the ACM and PM fields. This suggests that the LBB-UBB and ORAC sediments are in a more tectonically active setting than the Madigan and SHIM sediments.



# Conclusion and Proposed Future Work and Techniques

Results from this pilot study have proved to be very encouraging. A composite section at DBS represents a transgressive/regressive suite with four distinctive geochemical units. The Tanami Group which hosts the DBS goldfield is interpreted to be a relatively deep water, below storm wave base, marine transgressive-aggradational package that hosts multiple higher order condensed sections. Higher order condensed sections within the transgressive-aggradational suite contain the ore zones within black carbonaceous shales and iron formations.

The basin appears to have two distinct geochemical provenances which appear at the bottom and top of the sequence. All of the units are cut by multiple dolerite dikes. The Killi Killi formation, inferred to be proximal to a basin fan, infills the basin which is situated on a dominantly passive continental margin.

The Callie Boudin Chert, which is currently used as a stratigraphic marker at DBS, is here interpreted as nodules formed by sub-seafloor redox fronts as the basin is filled.

New techniques for this study have been developed successfully, creating a 'proxy' gamma curve from whole rock geochemistry. While the proxy gamma curve is helpful at highlighting some mineralised zones the addition of the  $\text{TiO}_2/\text{Zr}$  ratio curve and vanadium curve helps further pinpoint mineralised zones. The TOC curve when complete is also expected to further highlight mineralised areas.

While the use of downhole geochemistry to calculate a proxy gamma curve is successful it is also very time consuming and gives rise to a blocky/incomplete log as samples are 5 metres apart. Use of wireline logs of exploration holes as well as downhole geology potentially provide a much faster and more efficient technique at resolving stratigraphy and potential ore hosts. Previous downhole gamma tests are ambiguous due to lack of available downhole geology.

While some structural problems, including unit thickness and possible fault repetitions still need to be addressed, the composite core helps elucidate the DBS stratigraphy.

Further composite cores are planned for the 2004 field season from Titania, Ground Rush and Coyote and possibly from limited field exposures in order to gain a regional overview of the area. It is planned to supplement the current composite log at DBS with further drill hole information. This information will then be integrated with geochronology in order to further constrain the timing of fluid flow. Fence diagrams can then be constructed highlighting potential ore hosting surfaces.

## Acknowledgements

This study could not have taken place without the support and enthusiasm of Newmont Australia. Special thanks to Geoff Lowe who provided Geoscience Australia with the initial opportunity to work with Newmont. Ian Bamborough and James Emslie from Newmont are thanked for their many useful discussions. All the core shed folk are thanked for their help and support in core layout and sampling. Andrew Crispe from the Northern Territory Geological Survey provided useful discussions and the NTGS is thanked for their logistical support in the project.



At Geoscience Australia, Peter Southgate, David Huston, and the North Australia Project provided extremely helpful discussions, advice and reviews. John Pyke, Bill Pappas, Liz Webber, Ken Heighway, Rachel Davenport and Ziqing Hong are thanked for their help with analyses. Inge Zeilinger is thanked for her help with entering all the geochemical data into Geoscience Australia's data bases and Megan Lech and Carmine Moscaritolo provided much useful advice on inputting data into Geolog.

## References

Bhatia, M., 1983, Plate tectonics and geochemical composition of sandstones: *Jour. Geology*, v.91 p. 611-627.

Bhatia, M., Crook KAW., 1986, Trace element characteristics of greywackes and tectonic setting discrimination of sedimentary basins. *Contrib. Mineral. Petrol.*, 02 181-193.

Clayton, C.J., 1986, The chemical environment of flint formation in Upper Cretaceous chalks. In: Sieveking G de G, Hart MB (eds) *The Scientific study of Flint and chert*: Cambridge University Press p. 43-54.

Coniglio, M., 1987, Biogenic chert in the Cow Head Group (Cambro-Ordovician), western Newfoundland: *Sedimentology* v.34, p. 813-823.

Cooper, J.A., Ding, P.Q. 1997, Zircon ages constrain the timing of deformation events in The Granites-Tanami Region, northwest Australia. *Australian Journal of Earth Sciences* 44: p. 777-787

Crispe, A.J., Vanderberg, L.C., Cross, A.J., 2002, Geology of the Tanami region. Northern Territory Geological Survey Record 2002-0003, Annual Geoscience Exploration Seminar (AGES) record of Abstracts.

Crook, K.A.W., 1974, Lithogenesis and geotectonics: the significance of compositional variation in flysch arenites (graywackes), in DOTT, R.H., Shaver (eds), *Modern and ancient geosynclinal sedimentation*: SEPM Spec. Pub. 19.p. 304-310.

Degens, E.T., 1965, *Geochemistry of sediments*: Prentice-Hall, Englewood Cliffs, N.J., 342p.

Emslie, J., 2003, Personal communication, Callie mine

Emslie, J., Voulgaris P., (in prep) *Geology of the Dead Bullock Soak mining lease, Tanami, Northern territory, Australia*. Mimeralium Deposita

Hesse, R., 1990, Origin of chert: Diagenesis of biogenic siliceous sediments. In: McIlreath, I.A., Morrow, D.W., (eds) *Diagenesis: Geological association of Canada*, Geoscience Canada Reprint Series 4, p. 227-251.

Hendrickx, M.A., Slater, K., Crispe, A.J., Dean, A.A., Vanderberg, L.C., Smith, J., 2000, Paleoproterozoic stratigraphy of the Tanami Region: regional correlations and relation to mineralization-preliminary results. Northern Territory Geological Survey record GS 2000-13, 66pp.

Knauth, L.P., 1979, A model for the origin of chert in limestone. *Geology* V. 7, p. 274 -277.



Peters, K.E., 1986, Guidelines for evaluating petroleum source rock using programmed pyrolysis. AAPG Bulletin, 70, 318-29.

Pyke, J., 2000, Minerals laboratory staff develops new ICP-Magpie Schist preparation method. AGSO – Geoscience Australia Research Newsletter 33:12-14

Roser, B.P., Korsch, R.J., 1986, Determination of tectonic setting of sandstone-mudstone suites using SiO<sub>2</sub> content and K<sub>2</sub>O/Na<sub>2</sub>O ratio. J.Geol., V. 94, pp. 635-650

Smith, M.E., Lovett, D.R., Pring, P.I., Sando, B.G., 1998, Dead Bullock Soak deposits. In: Berkman, D.A., Mackenzie, D.H., (eds) Geology of Australia and Papu New Guinean deposits. The Australasian Institute of Mining and Metallurgy, Melbourne, pp. 449-460.

Taylor, S.R., and McLennan, S.M., 1985, The continental crust: its composition and evolution: Blackwell Scientific, Melbourne, 312 p.

Middleton, C.V., 1960, Chemical composition of sandstones: Geol.Soc. America Bull., v.71 p. 1011-1026

Norrish, K., Chappell, B.W., 1977, X-ray fluorescence spectrometry, *in*, Zussman, J.ed., Physical methods in determinative mineralogy: Academic Press, London, p.201-272.

UNSEAR., 1988. Exposures from Natural Sources of Radiation, Report, United Nations Scientific Committee on The effects of Atomic Radiation, New York

Vanderberg, I.C., Hendrickx, M.A., Crispe, A.J., 2001, Structural geology of the Tanami Region. Northern Territory Geological Survey Record 2001-004, 28pp

Williams, N.C., 2002, Controls on mineralisation at the Callie lode deposit, Tanami Desert, Northern Territory, Minerals and Geohazards Division, Geoscience Australia, Canberra, Geoscience Australia Professional Opinion 2002/09.

Whitaker, E., 2004, Communication via Geoff Lowe, Newmont Australia, after AGES 2004 conference

Wyborn, L.A.I., Chappell, B.W., 1983, Chemistry of the Ordovician and Silurian greywackes of the Snowy Mountains, southeastern Australia: An example of chemical evolution of sediments with time. Chemical Geology v. 39: p. 81 - 92



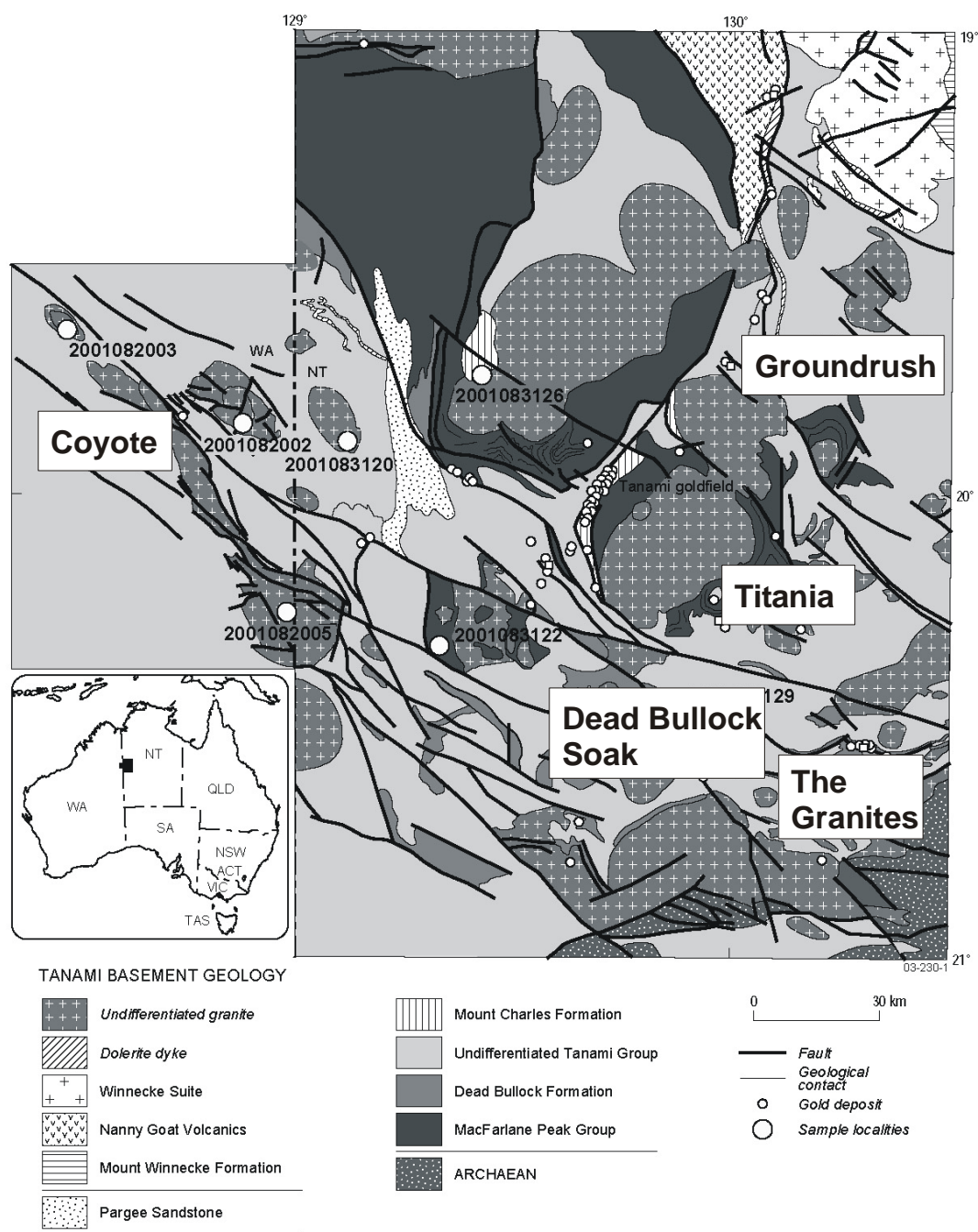


Figure 1. Location map showing the position of Dead Bullock Soak, The Granites, Groundrush, Titania and Coyote within the Northern Territory and Western Australia.



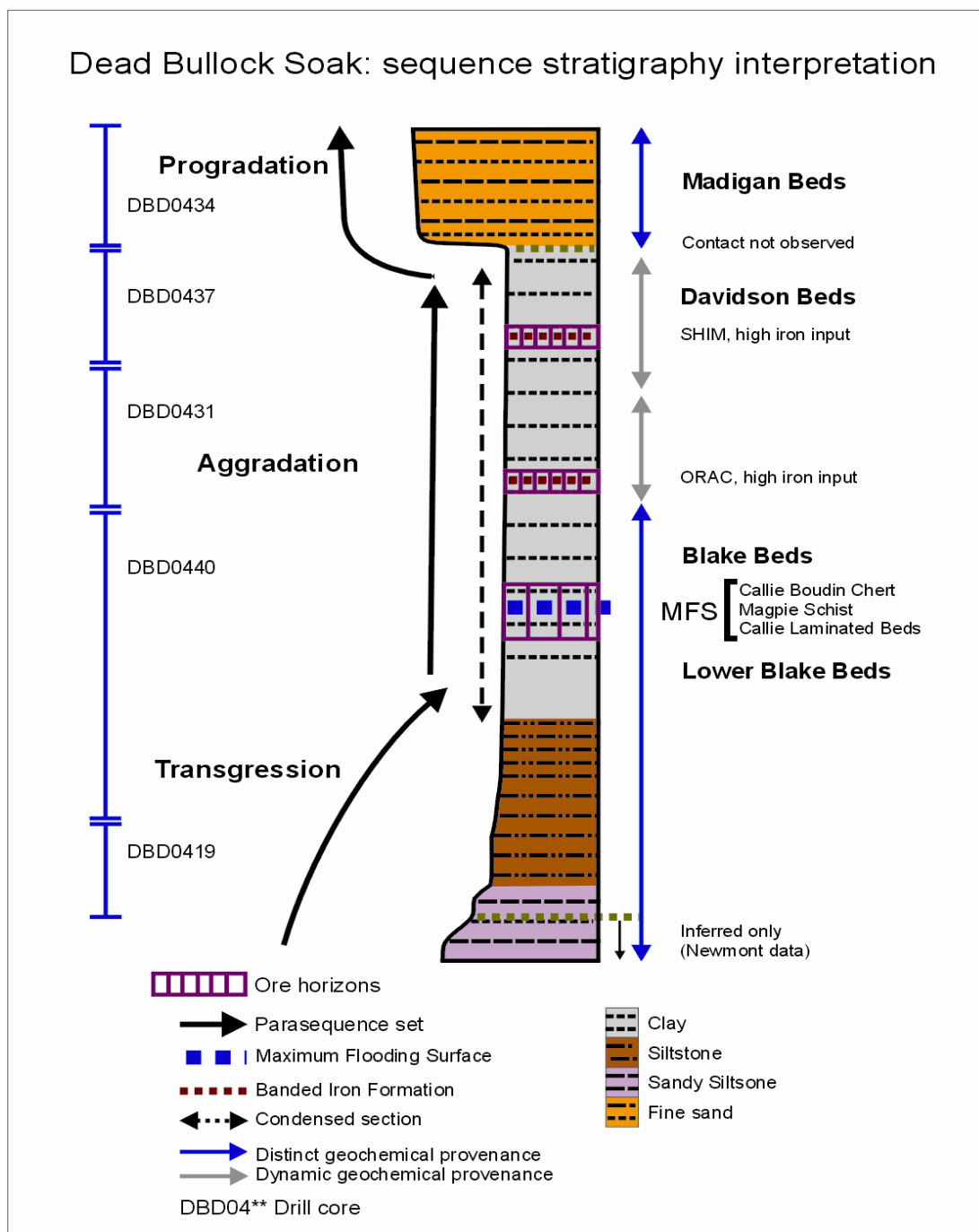


Figure 2. Schematic of the composite core at DBS. The composite core is made up of a transgressive, aggradational and progradational suite from a relatively deep water environment below storm wave base. The ore is found in the Maximum flooding surface and higher order Flooding surfaces.



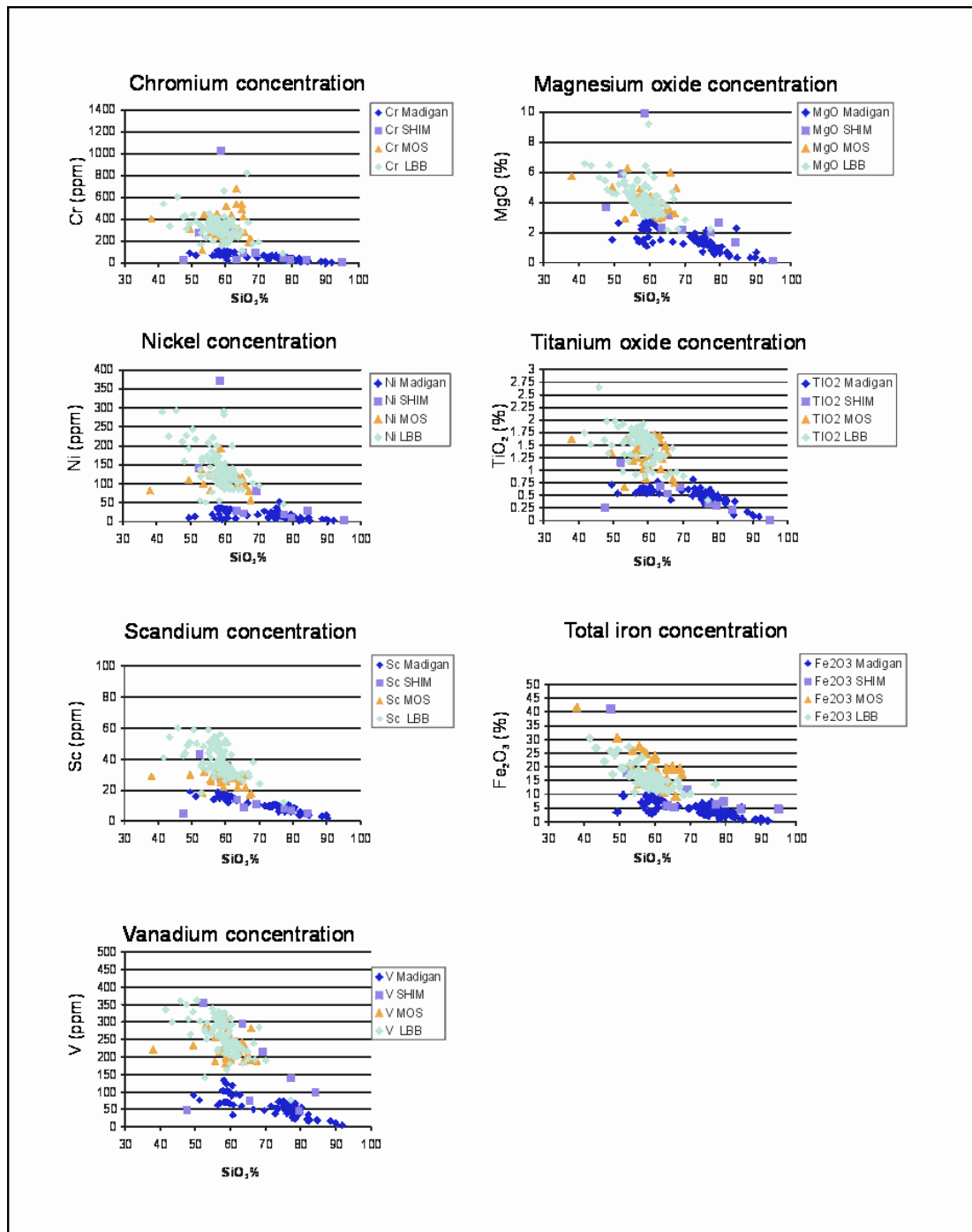


Figure 3. Chromium, nickel, scandium, vanadium, magnesium oxide, titanium oxide and total iron plotted versus silica. The four distinctive groups based on geochemistry are: 1) the basal group, LBB-UBB, which includes the LBL, LBB, CLB, MS, CBC and UBB; 2) the ORAC group is made up of the LOS, LOC, MOC, UOC and UOS; 3) the SHIM group includes the DBM, SHIM, CS, MC and SSS; and 4) the Madigan group, is the highest group in the stratigraphy and is made up of the Madigan Beds. Distinctive bipartite groups are observed for all the graphs, the Madigan data generally has lower values than the LBB-UBB group suggesting a change in provenance for the units.



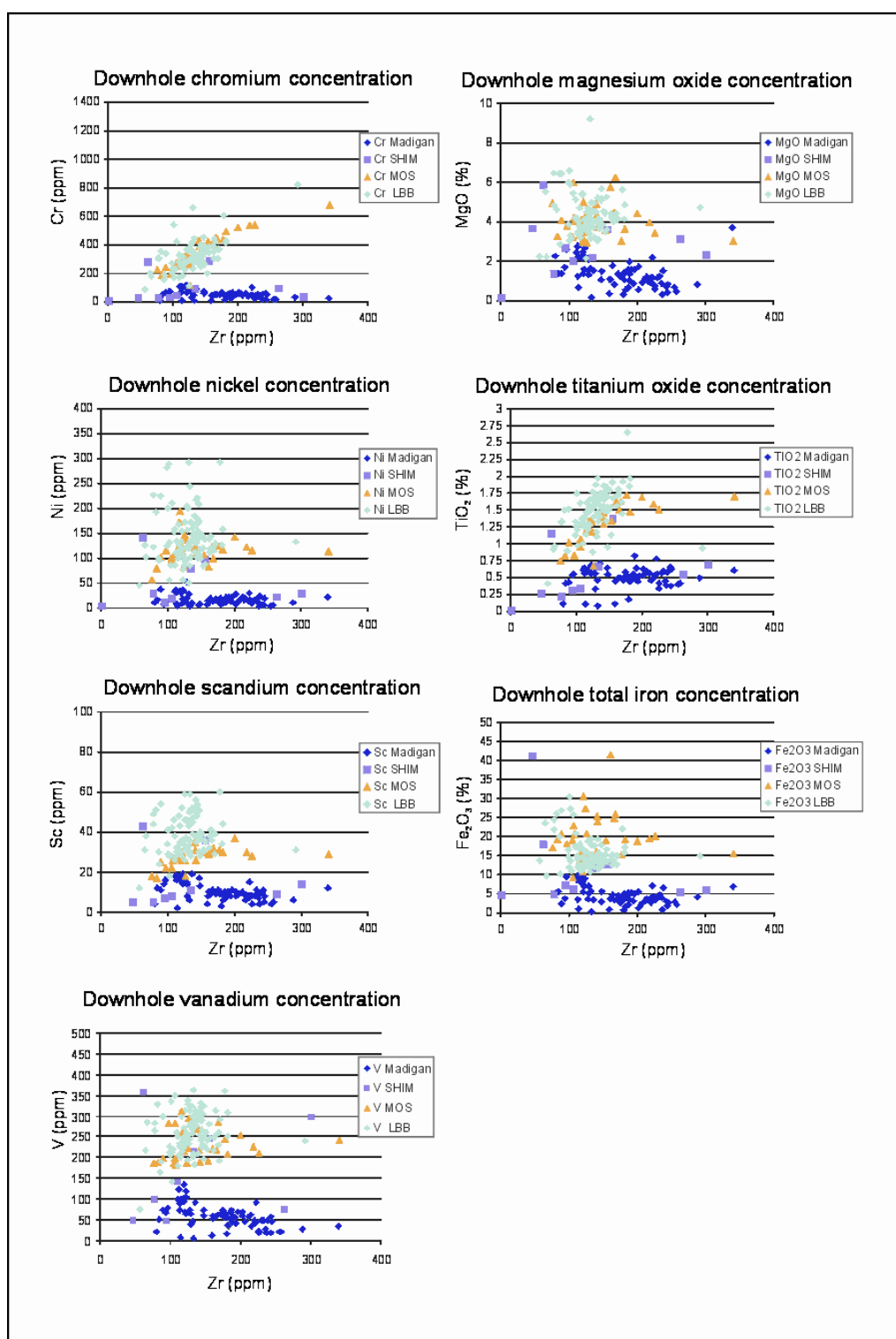


Figure 4. Chromium, nickel, scandium, vanadium, magnesium oxide, titanium oxide and total iron plotted versus zirconium. Traditionally all elements and traces are plotted to SiO<sub>2</sub> to gain an understanding of provenance but at Callie SiO<sub>2</sub> appears to be mobile as numerous quartz veins crosscut core. Zirconium at Callie is treated as immobile and is found to correspond well with the traditional silica provenance plots. Plots are plotted in order of grouped downhole stratigraphy similar to Figure 3.



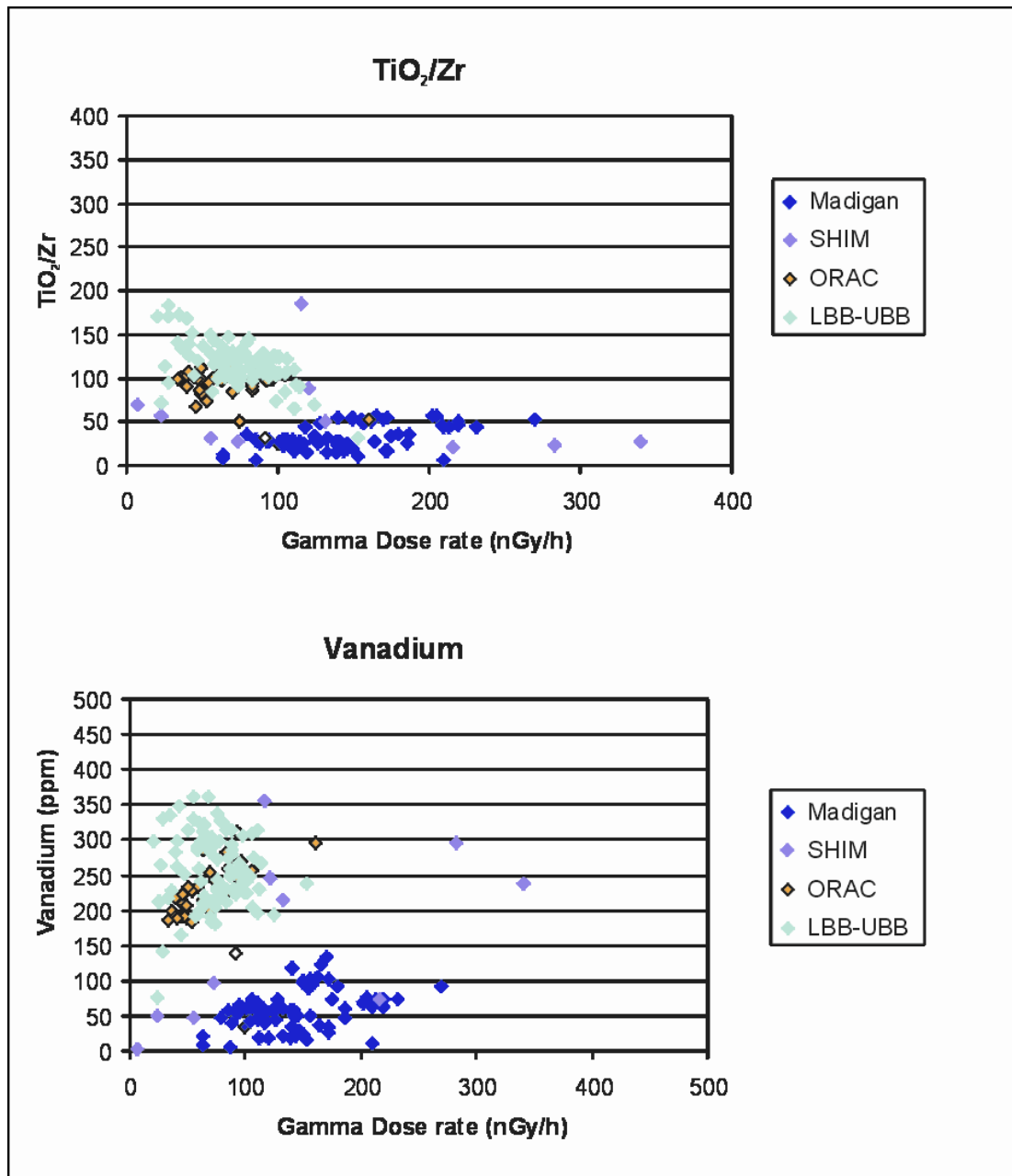


Figure 5. TiO<sub>2</sub>/Zr versus gamma for groups (Madigan – LBB-UBB) show a distinctive bipartite plot with the Madigan and SHIM groups having lower TiO<sub>2</sub>/Zr values than the UBB-LBB and ORAC groups. The same pattern plot is observed for the gamma versus vanadium with the Madigan Beds having distinctively lower vanadium values than UBB-LBB.



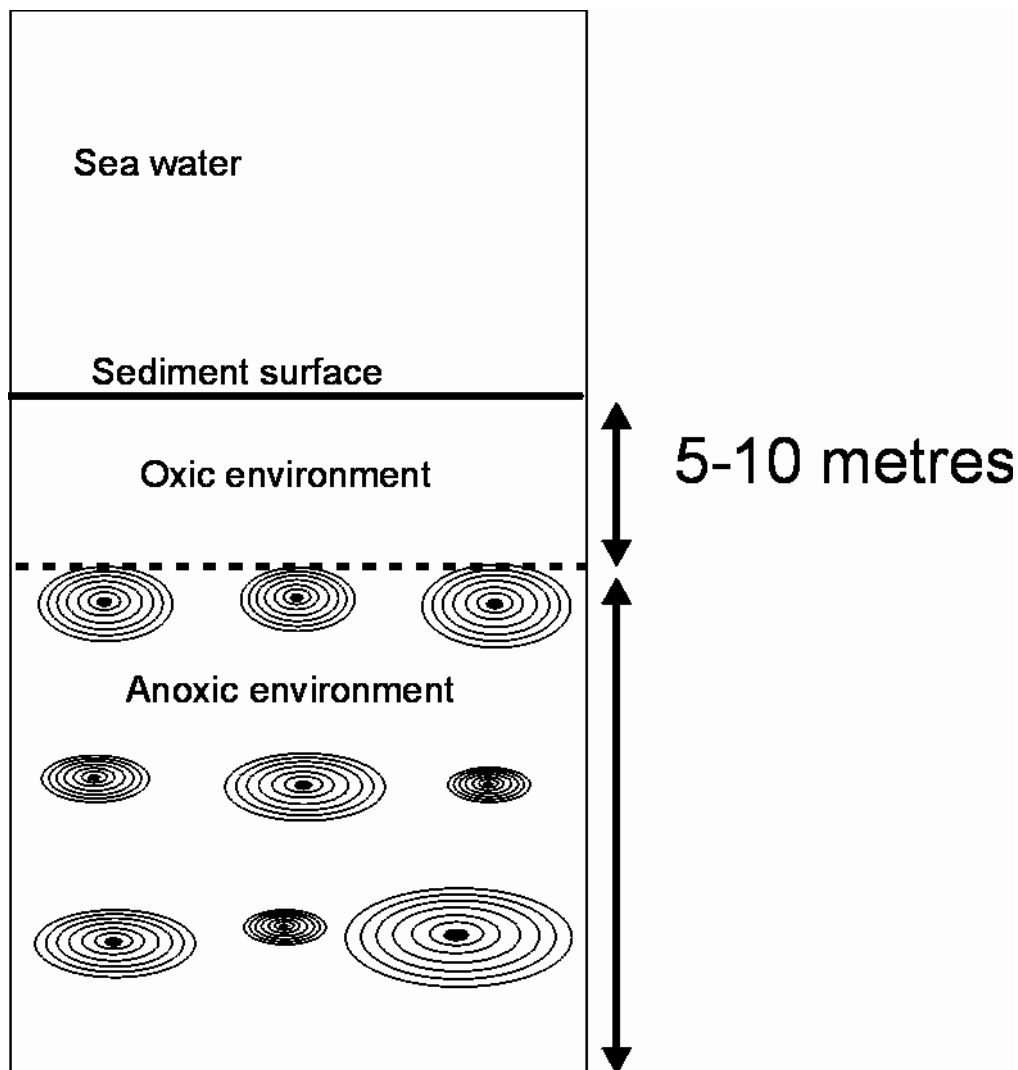


Figure 6. Clayton's (1986) model shows an explanation to explain the growth of nodules in sediment. The model shows the transition from anoxic to oxic conditions appears to coincide with the cemented chalk/flint boundaries and the flint bands mark the position of the redox boundary which separates an oxic (above) from an anoxic environment (below) at the time of silica precipitation. Assuming the model by Clayton we can use this as an explanation of the Callie Boudin Chert which is marking the redox boundary between anoxic and oxic environments. The nodules layers could form at times of low sediment input into the basin suggesting they are forming higher order condensed sections within the sequence. The nodules occur throughout the sequence at Callie, except in the Madigan Beds, so using the CBC as a diagnostic marker at Callie is perhaps enigmatic.



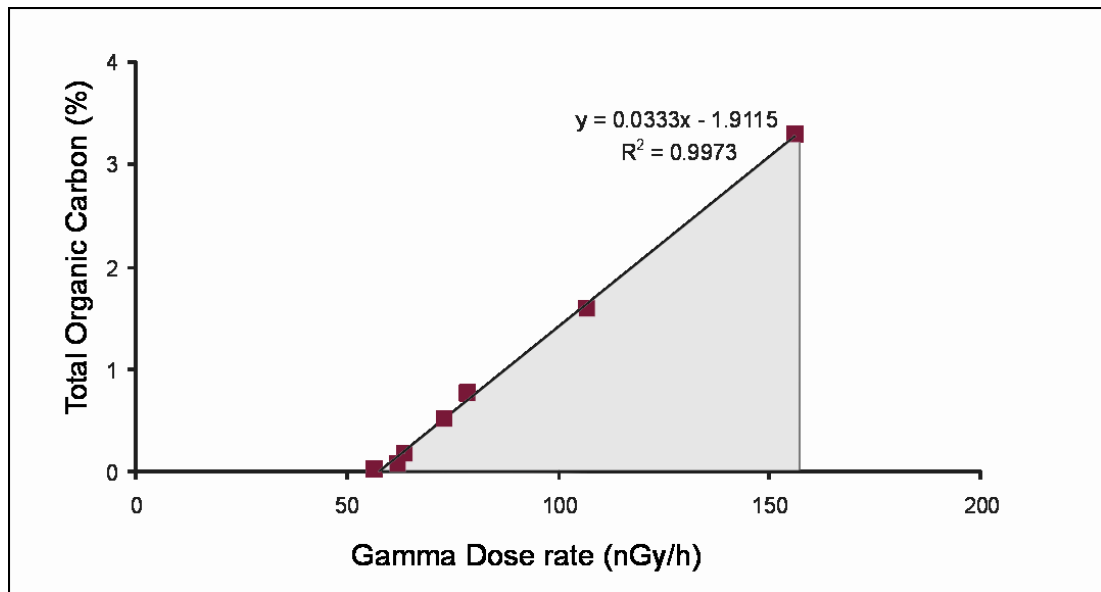


Figure 7. A pilot study was conducted to see if total organic carbon (TOC) could be used on samples from the Proterozoic. Seven samples from drill core DBD0440 taken from a siltstone grading into a black carbonaceous unit show high correlation between observed colour, and recorded TOC samples ranging from 0.04 % TOC for dull grey colour rocks to 3.3 % TOC for deep black colours. In this figure TOC is plotted against gamma and high correlation is observed. As mineralised units are approached the carbon value drops and gamma counts will potentially rise due to mobile potassium associated with mineralisation. This hypothetical window is depicted in the shaded area, where samples of lower TOC and gamma would plot.

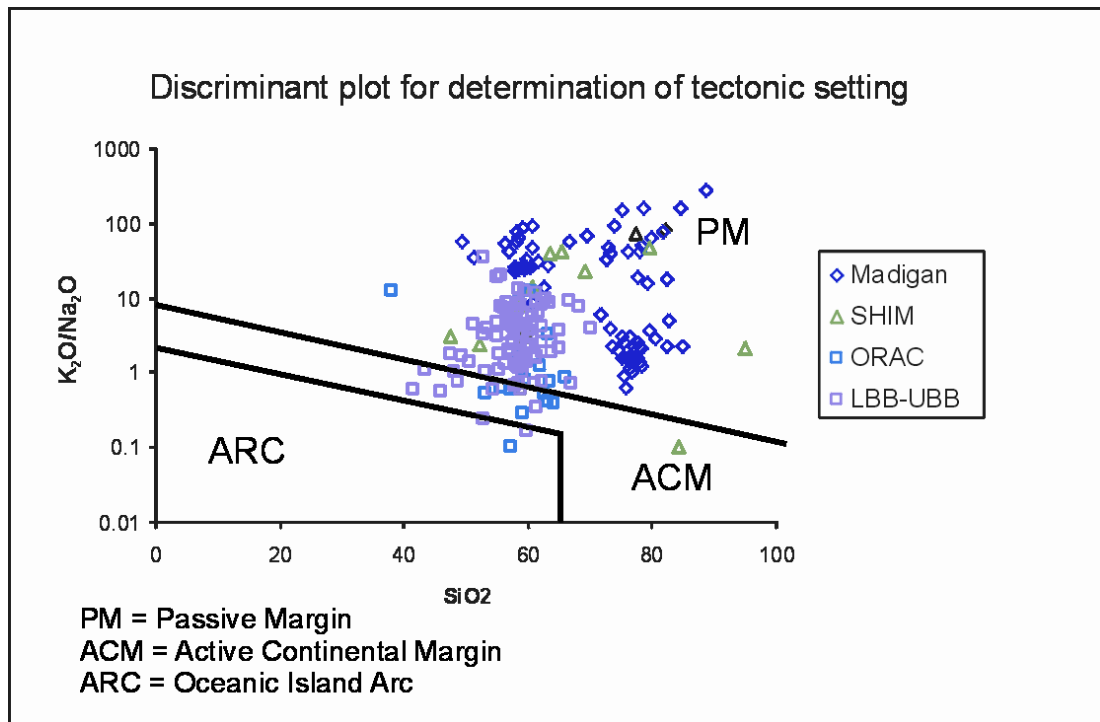


Figure 8. Divisions between areas on graphs are based on Roser and Korsch (1986): Passive continental margin (PM) form mineralogically mature (quartz-rich) sediment deposited in plate interiors away from active plate boundaries deposited within stable continental margins and basins. Active continental margin (ACM) are quartz-intermediate sediment derived from tectonically active continental margins or adjacent to active plate boundaries. Oceanic Island Arc (ARC) are quartz-poor volcanogenic sediments derived from uplifted areas associated with strike-slip faults and deposited in pull apart basins. The Madigan Beds display geochemistry that is largely consistent with Passive Margins, the Dead Bullock Soak Formation falls in a slight overlap with Passive Margins and Active Continental Margins, the samples in ARC are dismissed due to weathering products.



NTGS Stratigraphy (Hendrickx 2000)	NTGS Stratigraphy (200-4)	Newmont Stratigraphy Beds	Newmont units	Lithology	Grainsize	Interpreted Environment
Killi Killi Formation	Killi Killi Formation	Madigan beds	Madigan beds	Medium sandstone to fine meta siltstone		Turbidites, proximal to basin fans, basin infilling
Dead Bullock Formation	Dead Bullock Formation	Davidson beds	Manganiferous cherts, MCH Colgate schist, CS	Thinly bedded, non graphitic/graphitic iron rich interbedded fine meta-siltstone		Contact not observed
Twigg Formation (lateral equivalent to either Killi or Dead Bullock Formation)	Callie Member		* Schist Hills iron member, SHIM	Thinly bedded, non graphitic/graphitic iron rich interbedded fine meta-siltstones.		Condensed section containing higher order iron-rich flooding surfaces
			Dead Bullock member, DBM	Thinly bedded, non graphitic/graphitic interbedded fine meta Siltstones.		
MacFarlane Peak Group	Ferdies Member		Coora dolerite, CD	Medium to coarse grained Dolerite.		Maximum flooding surface within CLB, MS, CBC.
			* Orac formation	Thinly bedded, non graphitic/graphitic iron rich interbedded fine meta-siltstones.		
		Blake Beds	Upper Blake beds, UBB	Fine meta-siltstone, occasional graphitic beds, rip-up features, soft sediment deformation.		
			Pip schist, PS Callie boudin chert, CBC * Magpie schist, MS * Callie laminated beds, CLB Lower Blake beds, LBB Lower Blake Laminations, LBL	Meta sandy siltstone grading up to mudstone.		
				Clay Siltstone Sandy Siltstone Fine sand		Proximal to basin fan.
						Inferred data

Table 1. Comparison between NTGS stratigraphy, and local stratigraphy recognised at Dead Bullock Soak, in which further subdivisions are made on geochemical grounds and sedimentary features. \*Mineralised beds.





Madigan	gamma dose rate (nGy/h)	vanadium (ppm)	TiO <sub>2</sub> /Zr
Max	269.4	134.00	57.27
Min	63.4	5.00	5.87
Avg.	141.2	58.36	32.26
St.Dev. n = 76	41.9	28.23	14.01
SHIM			
Max	340.3	356.0	185.9
Min	6.9	1.5	20.4
Avg.	132.5	160.0	55.5
St.Dev. n = 11	105.8	116.4	48.3
ORAC			
Max	160.4	312.0	114.7
Min	33.3	183.0	49.9
Avg.	65.0	230.0	93.0
St.Dev. n = 30	27.3	36.9	15.4
UBB-LBB			
Max	152.5	362.0	182.8
Min	21.0	76.0	32.1
Avg.	75.7	256.8	116.4
St.Dev. n = 101	24.3	49.4	22.7

Table 2. Gamma dose rates (nGy/h), vanadium values (ppm) and TiO<sub>2</sub>/Zr values (ppm) for groups (Madigan – LBB-UBB) show a distinctive bipartite distribution with the Madigan and SHIM groups having lower TiO<sub>2</sub>/Zr values than the UBB-LBB and ORAC groups. The same pattern is observed for the gamma and vanadium values with the Madigan beds having distinctively lower vanadium values than the UBB-LBB.

Group 1 – Madigan Group	Madigan Beds
Group 2 – SHIM Group	Seldom Seen Schist, Manganiferous Cherts, Colgate Schist, Schist Hills Iron Member and Dead Bullock Member.
Group 3 – ORAC Group	Lower Orac Chert, Lower Orac Schist, Mid Orac Chert, Upper Orac Chert and Upper Orac Schist
Group 4 – LBB – UBB Group	Lower Blake Lode, Lower Blake Beds Callie Laminated Beds, Magpie Schist Callie Boudin Chert and Upper Blake Beds

Table 3: The data were clustered into four distinctive geochemical groups; each group shows distinctive geochemical characteristics as shown in Figure 3 and 4.



Madigan	Cr ppm	Nb ppm	Ni ppm	Sc ppm	Th ppm	V ppm	Y ppm	Ba ppm	Zr ppm	Fe2O3 %	SiO2 %	Al2O3 %	MgO %	MnO %	P2O5 %	TiO2 %
Max	115.00	52.00	52.00	19.00	27.00	134.00	54.00	1349.00	340	9.732112	91.92	33.44	3.71	0.328631	0.18	0.82
min	7.00	2.00	3.00	1.00	5.00	5.00	13.00	53.00	80	0.342541	49.51	4.71	0.15	0.019531	0.04	0.08
Avg.	57.58	14.34	17.96	10.54	17.62	58.36	28.79	538.75	173.2632	4.699046	71.94	15.91	1.41	0.068633	0.12	0.51
St.Dev.	29.01	6.23	10.28	4.63	4.96	28.23	8.10	265.85	53.21037	2.436325	10.07	6.30	0.70	0.05686	0.03	0.14
n 76																
SHIM																
Max	1029.00	31.00	371.00	43.00	47.00	356.00	68.00	2421.00	647	41.15916	95.00	20.85	9.91	0.610076	1.96	1.72
min	7.00	0.50	1.00	1.00	0.50	1.50	1.00	11.00	1	4.665177	47.59	0.15	0.14	0.023306	0.03	0.01
Avg.	71.22	14.96	25.11	11.52	17.68	70.74	28.62	575.72	172.9802	6.368878	68.48	15.88	2.59	1.065467	1.12	1.49
St.Dev.	299.08	8.61	108.30	13.90	16.79	116.40	18.18	645.66	181.1998	10.63365	14.30	6.46	2.62	0.174065	0.57	0.54
n 11																
ORAC																
Max	681.00	14.00	194.00	37.00	13.00	312.00	33.00	1007.00	341	41.54795	67.61	17.49	6.27	0.188883	0.28	1.72
min	118.00	6.00	57.00	17.00	3.00	183.00	13.00	5.00	76	9.187386	38.02	9.38	2.94	0.032413	0.04	0.67
Avg.	351.73	10.27	115.30	27.17	7.10	230.00	21.87	228.13	142.5	19.83688	59.49	12.77	4.05	0.095203	0.10	1.27
St.Dev.	126.10	1.76	26.72	4.65	2.20	36.92	4.61	238.38	53.24164	6.331835	5.96	2.20	0.89	0.04207	0.06	0.29
n 30																
UBB																
Max	824.00	15.00	293.00	60.00	26.00	362.00	43.00	1493.00	292	30.45035	77.21	22.60	9.22	0.172398	0.90	2.65
min	87.00	5.00	46.00	12.00	0.50	76.00	9.00	5.00	57	9.772954	41.63	6.40	2.15	0.033352	0.05	0.41
Avg.	319.68	9.58	139.84	38.59	8.09	256.75	24.49	406.36	130.6337	15.26264	58.25	17.17	4.25	0.075732	0.10	1.49
St.Dev.	101.81	1.99	50.14	9.44	4.05	49.44	5.40	273.03	29.89974	3.916424	5.05	2.42	1.01	0.030033	0.09	0.31
n 101																

Table 4. Statistics according to groups (Madigan – LBB-UBB) for chromium, niobium, nickel, scandium, thorium, vanadium, yttrium, barium, zirconium, total iron, aluminium oxide, magnesium oxide, manganese oxide, lead oxide and titanium oxide.

